LITERATURE CITED

1. M. G. Semena et al., "Investigation of the thermophysical characteristics of low-temperature heat pipes with metal-fiber wicks," Inzh. -Fiz. Zh., 31, No. 3 (1976).
2. A. S. Berkman and I. G. Mel'nikova, Porous Permeable Ceramics [in Russian], Izd.-vo Lit. po Str-vu, Leningrad (1969).
3. A. A. Zelengur and V. N. Mamonov, Poroshk. Metall., No. 11 (1969).
4. S. A. Druzhinin, Poroshk. Metall., No. 7 (1966).
5. E. P. Dyban, E. A. Maksimov, V. S. Pugin, and M. V. Stradomskii, Poroshk. Metall., No. 8 (1968).
6. N. S. Lidorenko, G. F. Muchnik, S. D. Solomonov, and A. R. Gordon, Teplofiz. Vys. Temp., 12, No. 5 (1974).
7. M. G. Semena, A. G. Kostornov, A. N. Gershuni, A. L. Moroz, and M. S. Shevchuk, Teplofiz. Vys. Temp., 13, No. 1 (1975).
8. S. V. Belov, Porous Metals in Engineering [in Russian], Mashinostroenie, Moscow (1976).

MAXIMUM HEAT FLUX IN PLANAR METAL-FIBER WICKS UNDER CONDITIONS TYPICAL OF HEAT PIPES

A. P. Ornatskii, M. G. Semena, and V. I. Timofeev

UDC 536.248.2

Experimental results of an investigation of the limiting heat flux for surfaces covered with a metal-fiber wick for different angles of inclination and variable length of the transport section are presented and discussed.

The investigation of evaporation and boiling of liquids on a plane surface covered with a metal-fiber wick gives a data base for elucidating the physical conditions for the heat-transfer process in the heat supply zone, and for choosing the optimal geometric and structural parameters of the wick. The capillary-transport properties of metal-fiber wicks were studied in [1-3], and the authors were able, to a first approximation, to optimize the structural parameters of materials made of baked discrete monodispersed fibers. However, to improve the method of designing heat pipes and heat-transfer agent distributions in film evaporators, additional investigations are required of the transport capabilities of metal-fiber wicks under heat-transfer conditions.

One of the most important characteristics of heat-transfer devices, including heat pipes, is the maximum heat flux transmitted under normal operating conditions.

The maximum heat flux Q_{max} in the heat zone of low-temperature heat pipes is very often a limit on the capillary transport of the heat-transfer agent [4-6], and depends on the structural and constructional characteristics of the porous material, the thermophysical properties of the working liquid, and also the heat pipe operating conditions.

The simultaneous solution of the equations of conservation of mass, energy, and momentum for an element of a metal-fiber wick [7] can be written in the form

$$Q_{max} = 4N \frac{k_w}{D_{ef}} \cdot \frac{F_w}{0.5(L_e + L_c) + L_a} \left(1 - \frac{\Delta P_g}{\Delta P_c}\right). \quad (1)$$

It can be seen from Eq. (1) that, for correct choice of the working liquid, to ensure a maximum value of the parameter $N = \sigma\rho_l r/\mu_l$, wicks characterized by good capillary-transport capabilities (a maximum of the parameter k_w/D_{ef} and of the capillary head ΔP_c) are more efficient. It is clear also that Q_{max} is affected by the cross-sectional area F_w of the wick, and the reduced filtration length $0.5 (L_e + L_c) + L_a$.

Kiev Polytechnic Institute. Translated from Inzhenerno-Fizicheskii Zhurnal, Vol. 35, No. 5, pp. 782-788, November, 1978. Original article submitted December 15, 1977.

0022-0841/78/3505-1272$07.50

TABLE 1. Characteristics of Metal-Fiber Wicks

Wick no.	Porosity Π, %	Thickness δ_w, mm	Effective pore diam. D_{ef}, μm	Parameter $k_w/D_{ef} \cdot 10^6$ m	Geometric dimensions, mm
1	60	1	60	0,94	500×45×1
2	60	2	60	0,94	450×45×2
3	60	3	60	0,94	500×45×3
4	70	2	60	1,21	450×45×2
5	80	1	110	3,31	450×45×1
6	80	2	85	2,26	500×45×2
7	80	2	110	3,31	450×45×2
8	80	2	65	0,87	500×45×2

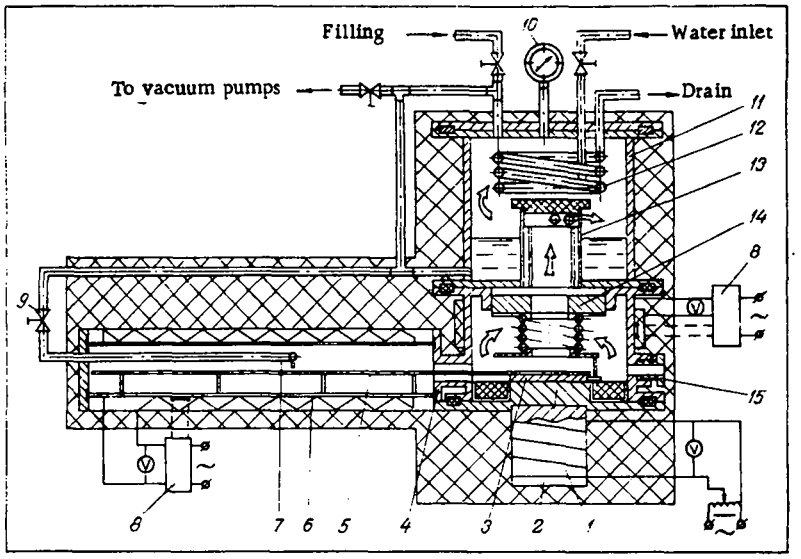

Fig. 1. Schematic of the experimental equipment: 1) electrical heater; 2) stainless steel block; 3) copper substrate; 4) evaporation chamber; 5) wick; 6) glass tube; 7) copper tube; 8) electronic temperature control circuit; 9) control valve; 10) vacuum manometer; 11) condensation chamber; 12) heat exchanger; 13) heat pipe; 14) spring device; 15) window.

The present authors have investigated the influence of these parameters on Q_{max} for wicks whose characteristic are shown in Table 1.

Experimental equipment was made up to simulate the operation of the actual heat pipe and in which one could investigate the heat-transfer process in the heater zone with capillary-porous structures in various liquids, for various saturation pressures, various lengths of the transport section, and various angles of inclination of the wick.

The experimental equipment (Fig. 1) consisted of a unit for supplying and measuring the heat flux, an evaporation chamber, and a condensation chamber, and it had a glass tube to locate the transport part of the wick. The heat flux in the evaporation chamber from the electrical heater was transmitted through the steel block to the copper substrate to which the test wick specimen was attached. A spring device in each case maintained a constant spring force of 6 ± 0.5 kgf/cm^2 pressing the substrate to the steel block; the device allowed specimens to be interchanged. The condensate of working liquid, generated at the outer surface of the heat exchanger, was supplied to the part of the wick located in the glass tube. A uniform supply of condensate along the wick was accomplished by means of a comb which could be moved along the length of the wick, varying the length of the transport section. The surface temperature of the glass tube and the evaporation chamber was maintained at the saturation temperature by means of an automatic temperature control system. This maintained adiabatic conditions for the transport section of the wick in the glass tube, and also eliminated possible condensation of the working liquid along the walls of the evaporation chamber. The temperature in the evaporation part of the wick was determined by means of four thermocouples, uniformly distributed

TABLE 2. Maximum Heat Flux Obtained in No. 2 Wick

Length of transport section L_a, mm	Angle of inclination φ, deg	Acetone	Ethanol
		max. heat flux Q_{max}, W	
125	0	78,5	64,5
	15	60,5	52,5
	30	48,4	36,3
	45	22,3	14,2
	90	10,1	—
175	0	54,5	46,3
	15	40,2	30,3
	30	16,2	12,1
250	0	40,2	36,3
	15	22,3	16,1
400	0	27,2	20,2

TABLE 3. Maximum Heat Flux Transmitted by the Test Wicks in Acetone

Wick no.	L_a, mm	φ, deg	Q_{max}, W	q_{lr}, W/cm^2	Wick no.	L_a, mm	φ, deg	Q_{max}, W	q_{lr}, W/cm^2
1	125	0	20,2	1,0	6	125	0	153	7,55
		15	15,1	0,75			15	97	4,8
	175	0	13,2	0,65			30	72,5	3,58
						175	0	109	5,4
3	125	0	131	6,5			15	60,5	3,0
		15	60,5	3,0			30	20,2	1,0
		30	46,5	2,3		250	0	65	3,21
	175	0	83,1	4,1			15	22,3	1,1
		15	32,5	1,6		400	0	46,5	2,3
	250	0	70,5	3,48					
		15	24,2	1,19	7	125	0	238	11,7
	400	0	46,5	2,3			15	117	5,8
							30	46,5	2,3
4	125	0	99	4,9		175	0	182	9,0
		15	58,5	2,9			15	80,8	3,98
		30	42,5	2,1		250	0	162	8,0
		45	22,1	1,09		400	0	80,8	3,98
	175	0	57,7	2,85	8	125	0	95	4,7
		15	46,5	2,3			15	75	3,7
		30	32,3	1,59			30	60,6	3,99
	250	0	36,3	1,79			45	32,4	1,6
		15	18,2	0,9		175	0	70,7	3,48
	400	0	20,2	1,0			15	52,5	2,6
							30	30,4	1,5
5	125	0	141	7,0		250	0	44,5	2,8
							15	20,2	1,0
	175	0	109	5,4			30	10,1	0,5
						400	0	28,3	1,4
							15	12,3	0,68

in the substrate at a distance of 0.5 mm from the point where it was welded to the wick. All the thermocouples were calibrated to an accuracy of ±0.1°K, along with the measurement system.

The heat flux was determined by means of three pairs of differential thermocouples, stamped into the steel block. The discrepancy in determining the heat flux from the power supplied and from the temperature drop in the calibration did not exceed ± 5%.

The limiting value Q_{max} was determined from the sharp increase in substrate temperature. The wall temperature t_{ss} is an average between the readings of the two thermocouples which are farthest from the zone in which the working liquid is supplied. Supply of working liquid to the filter from the condensation chamber was accomplished by means of a throttle valve, and corresponded to the flow rate of evaporating liquid. The investigations were conducted at constant pressure P = 400 torr in the evaporating chamber.

Acetone and ethanol were the working liquids used.

Analysis of the results in Table 2 shows that acetone is a more efficient heat-transfer agent in comparison with ethanol. This is due to the fact that the parameter N for acetone is larger than for ethanol (e.g., for t_s = 40°C $N_{ac} = 31.5 \cdot 10^5$ W/cm^2, $N_{et} = 20 \cdot 10^5$ W/cm^2). The data of Tables 2 and 3 also indicate that Q_{max} depends appreciably on the angle of inclination φ of the specimen filters to the horizontal (the heating zone is

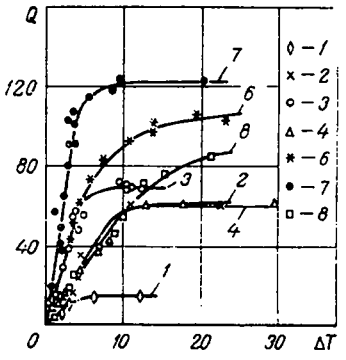

Fig. 2

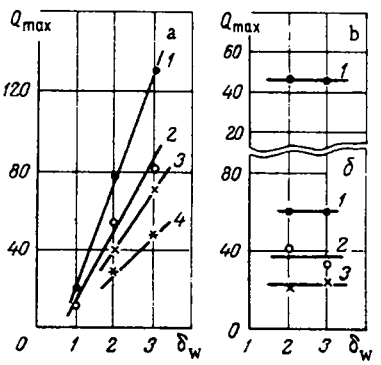

Fig. 3

Fig. 2. Typical shape of the relation $Q = f(\Delta T)$ for acetone with φ = 15° and L_a = 125 mm. The numbers on the curves and the points show the wick number.

Fig. 3. The limiting heat flux as a function of wick thickness: a) φ = 0°; b) 15°; c) 30°; 1) L_a = 125 mm; 2) 175; 3) 250; 4) 400.

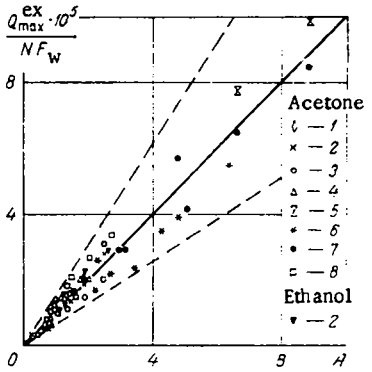

Fig. 4. Comparison of the experimental values of Q_{max} with those calculated using Eq. (1): 1-8) wick number; $A = [4K_w \cdot 10^5 / D_{ef} L_{lt}] (1 - \Delta P_g / \Delta P_{cap})$.

above the liquid supply zone) and the length of the liquid transport section L_a. However, with appropriate choice of working liquid, structural parameters and filtration length, metal-fiber wicks can operate in heat pipes against the force of gravity (e. g., No. 2 with L_a = 125 mm in acetone).

The values of Q_{max} shown in Tables 2 and 3 were determined graphically from graphs of the functions $Q = f(\Delta T)$. Figure 2 shows a typical correlation of the heat flux supplied as a function of the temperature drop $\Delta T = t_{ss} - t_s$ for all the test wicks in acetone with L_a = 125 mm and φ = 15° (operating against the force of gravity). Because the metal-fiber wicks have good thermal conductivity and active open porosity, the limit of normal function of the wicks sets in smoothly, without abrupt discontinuities in wall temperature.

All the limiting values of Q_{max} in this investigation were reached by limiting the capillary-transport capability of the wick. This was shown by visual observation, and also by the fact that the limiting heat flux increased sharply when the wick specimen was inclined.

Visual observations and photographs were not able to determine the attainment of limiting heat flux, and therefore, the value of Q_{max} was determined graphically in this investigation, corresponding to the beginning of departure from the bubble boiling curve. The relative error in determining Q_{max} is ± 15%. However, the visual observations made it possible to fix the transition from the evaporating to the bubble boiling regime, with horizontal location of the wick (φ = 0 ± 5°) (the appearance of vapor bubbles at the wick surface for a heat

flux density of q = 0.5-1 W/cm^2, and the formation of vapor channels with further increase in the heat flux), and also to observe fluctuations of liquid in the wick and the drying out process. The slope of the function $Q = f(\Delta T)$, also equal to $q = f(\Delta T)$, depends on the structural characteristics of the wick, and primarily on the effective pore diameter D_{ef}. For example, Wicks Nos. 7 and 8, which have the same porosity $\Pi = 80\%$ and thickness $\delta = 2$ mm, differ appreciably in the slope of the curve, since they differ in the quantity D_{ef} by almost a factor of 2 (Fig. 2).

The influence of wick thickness δ_w on the limiting heat flux is shown in Fig. 3, which gives values of Q_{max} Nos. 1, 2, and 3 with the same porosity $\Pi = 60\%$ and effective pore diameter $D_{ef} = 60\ \mu$. With increase of δ_w and horizontal location (Fig. 3a) the maximum heat flux increases, as follows from Eq. (1). However, for angles of inclination such that the wick operates against gravity this increase is practically imperceptible, since, when the heater zone is raised above the condensation zone, the main pores are not in a state to retain liquid, because of the nonuniformity of the pore dimensions, and thus, the effective thickness of the wick decreases (Fig. 3b, c).

With horizontal operation of the wicks a single-valued monotonic dependence of Q_{max} on the parameter k_w/D_{ef} is observed (e.g., for wicks Nos. 8, 4, 7, with thickness $\delta_w = 2$ mm and $L_a = 125$ mm, Q_{max} and k_w/D_{ef} are 95, 99, and 238 W and $0.87 \cdot 10^6$; $1.21 \cdot 10^6$; $3.31 \cdot 10^6$ m, respectively). In the case when the heater zone is raised, the mutual influence of the parameters k_w/D_{ef} and the ratio $\Delta P_g/\Delta P_{cap}$ have an influence on Q_{max}, and the function becomes uniquely dependent on k_w/D_{ef}. For the wicks investigated, an increase in Q_{max} with increase of k_w/D_{ef} is observed only up to an inclination angle of $\varphi = 20 \pm 5°$. Further elevation of the evaporating section above the liquid supply zone leads to a decrease in Q_{max} with increase in k_w/D_{ef}.

Figure 4 compares the experimental data obtained on the maximum heat capability of Wicks Nos. 1-8 in acetone and ethanol, in the heater zone, $Q_{max} \cdot 10^5/N F_w$, with the result of an analytical determination of $4K_w/D_{ef}L_{lt}(1 - \Delta P_g/\Delta P_{cap})$. The physical constants of the working liquid required for the calculation were determined from the saturation temperatures at a pressure of p=400 torr in the equipment. In the calculation $L_{lt} = 0.5\ L_e + L_a$ [8], since the condensation zone was immersed in the working liquid and did not take part in the heat-transfer agent filtration circuit. As can be seen from Fig. 4, the deviation of experimental data from theory does not exceed ±35%.

NOTATION

Q	is the heat flux transmitted, W;
σ	is the surface tension, N/m;
k_w	is the permeability, m^2;
F_w, δ_w	are the cross section and thickness of the wick, m^2 and mm;
D_{ef}	is the effective pore diameter, μm;
r	is the latent heat of evaporation, J/kg;
μ_l	is the dynamic viscosity, N · sec/m^2;
ρ_l	is the density, kg/m^3;
L_e	is the length of evaporator, m;
L_a	is the length of adiabatic zone, m;
L_c	is the length of condenser, m;
ΔP_g	is the gravitational head, N/m^2;
ΔP_{cap}	is the capillary head, N/m^2;
N	is the parameter accounting for the properties of the working liquid, W/cm^2;
q	is the heat flux density, W/cm^2;
T_s and t_s	are the saturation temperature, °K, °C;
ΔT	is the temperature drop, °K;
φ	is the angle of wick inclination, deg;
Π	is the porosity, %.

Subscripts

max	is the maximum;
ss	is the substrate;
lt	is the limit;
ac	is the acetone;
et	is the ethanol.

LITERATURE CITED

1. M. G. Semena et al., Inzh.-Fiz. Zh., 27, No. 6 (1974).
2. M. G. Semena et al., Teplofiz. Vys. Temp., 13, No. 21 (1975).
3. M. G. Semena et al., Inzh.-Fiz. Zh., 28, No. 22 (1975).
4. M. G. Semena et al., Inzh.-Fiz. Zh., 31, No. 23 (1976).
5. I. K. Ferrel, E. G. Alexander, and W. T. Piver, "Vaporization heat transfer in heat pipe wick materials," AIAA Paper 72-256 (1972).
6. Ferrel and Johnson, Heat Transfer Mechanism in the Evaporation Zone of a Heat Pipe. Heat Pipes [Russian translation], Mir (1972).
7. C. H. Cosgrove, I. K. Ferrel, and A. Carnesale, "Operating characteristics of capillary-limited heat pipes," J. Nucl. Energy, 21, No. 7 (1967).
8. K. T. Feldman and C. C. Roberts, "Predicting performance of heat pipes at high heat flux," Fourth International Congress, D 3.6, Prague (1972).
9. I. C. Corman and G. E. Walmet, "Vaporization from capillary wick structures," ASME Paper HT-35 (1971).

TWO-DIMENSIONAL LAMINAR BOUNDARY LAYER IN FLOW OF THERMODYNAMICALLY EQUILIBRATED WATER VAPOR

R. A. Rakhimzyanov and V. G. Zharinov

UDC 533.6.01

This paper examines the boundary problem of a laminar boundary layer in flow of thermodynamically equilibrated water vapor. An approximate method of solution is proposed, based on an approximation for the density and the coefficient of dynamic viscosity across the layer.

At present only experimental investigations are known of flow in a boundary layer formed in a nozzle with motion of water vapor [1, 2]. In particular, it is noted that the boundary layer in a Laval nozzle, when it has spontaneous condensation, when the liquid phase is finally dispersed, consists of two sublayers: an upper vapor-drop layer and a lower heated vapor layer (adjacent to the wall).

Below we present results of a theoretical investigation of flow in a two-dimensional laminar boundary layer with motion of water vapor along a solid impermeable surface.

Statement of the Problem. For the water vapor we assume that the liquid phase is in a finely dispersed state and that the velocities of the phases are the same: the thermodynamic equilibrium of the phases is not perturbed, and the temperature and pressure obey the vapor pressure curve. With these assumptions water vapor can be regarded as some kind of imperfect gas.

In considering the equations of motion and continuity of the laminar boundary layer, derived, e.g., in [3], no assumptions of any kind are made concerning the gas being perfect. Therefore, these equations will be valid in our case.

Having made the transformations usually applied in boundary layer theory, we obtain the energy equation for a two-dimensional steady-state laminar boundary layer in an imperfect gas

$$\rho u \frac{\partial h}{\partial x} - \rho v \frac{\partial h}{\partial y} = u \frac{dp}{dx} - \mu \left(\frac{\partial u}{\partial y}\right)^2 - \frac{\partial}{\partial y}\left(\lambda \frac{\partial T}{\partial y}\right).$$

To determine the dynamic viscosity of a two-phase medium we use the "Einstein correction" [3]:

$$\frac{\mu}{\mu_v} = 1 - m \frac{\mu_l - 2{,}5\mu_l}{\mu_v - \mu_v},$$

Translated from Inzhenerno-Fizicheskii Zhurnal, Vol. 35, No. 5, pp. 789-795, November, 1978. Original article submitted November 25, 1977.

0022-0841/78/3505-1277 $07.50